ChemComm

Simultaneous production of hydrogen and chlorine through overall brine splitting with a particulate photocatalyst

Journal:	*ChemComm*
Manuscript ID	CC-COM-01-2024-000136.R1
Article Type:	Communication

COMMUNICATION

Simultaneous production of hydrogen and chlorine through overall brine splitting with a particulate photocatalyst

Received 00th January 20xx,
Accepted 00th January 20xx

DOI: 10.1039/x0xx00000x

Takumi Okada,[ab] Masanori Kodera,*[a] Yugo Miseki,[a] Hitoshi Kusama,[a] Takahiro Gunji [b] and Kazuhiro Sayama *[ab]

Sunlight-driven photocatalytic water splitting shows promise for green H_2 production. In an attempt to achieve seawater splitting, we constructed a new stoichiometric brine splitting system that produces H_2 along with Cl_2 instead of O_2. Cl_2—a more potent high-value-added oxidant than O_2—was obtained with 100% selectivity over 10 h by adjusting the solution pH to acidic using a UV-light-driven Pt-loaded TiO_2 photocatalyst. Our new photosynthesis system can permit economically feasible solar chemical production.

Global warming driven by greenhouse gas emissions, which has become a critical issue for modern society, must be mitigated by transitioning from fossil fuels to renewable energy sources.[1,2] However, renewable energy is typically transformed into chemical energy for storage and transportation. In this context, the conversion of solar energy to green and inexpensive H_2 from water using particulate photocatalysts has garnered considerable attention.[3]

Fresh water is crucial for ingestion and agriculture, and is sometimes considered a precious resource in developing countries and remote islands.[4] Therefore, seawater and brine, which constitute over 97% of the water on Earth, are worth investigating in this regard.

Seawater contains ~500 mM Cl^- ion, which participates in oxidation reactions as well as H_2O. Evidently, Cl^- ion oxidizes to form chlorine (Cl_2), hypochlorous acid (HClO), and hypochlorite ion (ClO^-) under acidic, neutral, and basic conditions, respectively (Fig. S1).[5] The standard redox potentials *vs.* reversible hydrogen electrode (V *vs.* RHE) for the seawater splitting reactions are provided below.

$$2H_2O \rightarrow O_2 + 4H^+ + 4e^-, \quad E = 1.23 \text{ V vs. RHE} \qquad (1)$$

$$2Cl^- \rightarrow Cl_2 + 2e^-, \quad E = 1.36 + 0.059 \times \text{pH V vs. RHE} \qquad (2)$$

$$Cl^- + H_2O \rightarrow HClO + H^+ + 2e^-, \quad E = 1.49 + 0.0295 \times \text{pH V } vs. \text{ RHE} \qquad (3)$$

$$Cl^- + H_2O \rightarrow ClO^- + 2H^+ + 2e^-, \quad E = 1.72 \text{ V } vs. \text{ RHE} \qquad (4)$$

Cl_2, HClO, and ClO^- are obtained *via* two-electron oxidation. Furthermore, they are considered equivalent from an electrochemical perspective, given their tendency to reversibly transform as follows:

$$Cl_2 + H_2O \leftrightharpoons HClO + HCl, \quad K = 3.94 \times 10^{-4} \text{ M}^2 \qquad (5)$$

Notably, O_2 is thermodynamically the most favorable product among the four aforementioned species at all pH values.

Most studies on the electrolysis of seawater or brine (containing NaCl) have focused on producing H_2 and O_2 by disregarding Cl^- ion oxidation,[6–8] which has resulted in HClO being considered an undesired byproduct. However, HClO is considered as a valuable chemical because it exhibits several attractive features. For instance, it is an extensively used oxidant for disinfecting potable water, bleaching, cleaning, deodorizing, treating dye wastewater, and sterilizing food because of its strong oxidizing power in aqueous solutions.[9–11] Furthermore, it has recently drawn attention as an antiviral agent against SARS-CoV-2. Consequently, HClO is several hundred times more expensive than O_2.[12] However, HClO decomposes gradually over time even in the dark; therefore, it is not conducive to prolonged storage, and consequently, on-site production at the usage location is preferred. Notably, on-site production eliminates the need for long-distance product transport and the product concentration methods typically adopted in conventional large-scale production schemes, making it an exceptionally realistic system that may be realized in the near future for generating useful products using

[a] *Global Zero Emission Research Center (GZR), National Institute of Advanced Industrial Science and Technology (AIST), Tsukuba West, 16-1, Onogawa, Tsukuba, Ibaraki, 305-8569 Japan*
[b] *Department of Pure and Applied Chemistry, Faculty of Science and Technology, Tokyo University of Science, 2641, Yamazaki, Noda, Chiba 278-8510, Japan*

† Electronic Supplementary Information (ESI) available: Experimental; potentials of Cl_2, HClO, ClO^-, and O_2; XRD pattern; e^-/h^+ ratio of products at pH 1; time courses monitored using a batch-type system; power spectra of the LED lamp; time courses obtained after re-evacuation; comparison of results obtained in this study with those of other brine splitting systems; DFT results. See DOI: 10.1039/x0xx00000x

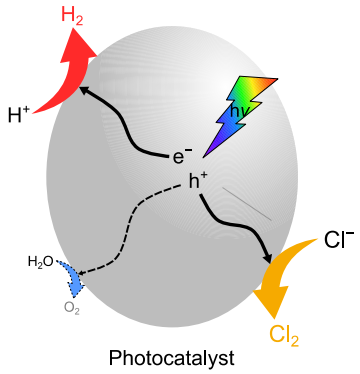

Fig. 1 Schematic illustrating the simultaneous production of H_2 and Cl_2 using a powdered photocatalyst.

photocatalysts. Therefore, simultaneous production of H_2 and HClO through on-site photocatalytic seawater splitting is worth exploring as an economically and practically feasible system (Fig. 1).

Recently reported photoelectrochemical HClO production schemes require a certain external bias.[13,14] Furthermore, photocatalytic HClO production from brine has been achieved by leveraging the O_2 reduction reaction and using powder-based photocatalytic systems (Eq. 2 and 6), which can be more readily scaled-up than photoelectrode systems.[15,16]

$$O_2 + 4H^+ + 4e^- \rightarrow 2H_2O, \quad E = 1.23 \text{ V } vs. \text{ RHE} \qquad (6)$$

Additionally, certain studies have implied the occurrence of partial Cl^- oxidation.[17,18] However, to our knowledge, intentional and selective production of H_2 and HClO in a stoichiometric ratio through brine splitting has not been reported to date. In this study, we devised an overall brine splitting process for concurrently producing H_2 and Cl_2 with a particulate photocatalyst. Pt-loaded TiO_2 photocatalysts helped generate H_2 and Cl_2 in a stoichiometric ratio under UV irradiation in an acidic medium. Our results underscore the potency of the newly formulated scheme as an artificial photosynthesis system.

Particulate TiO_2 with 0.1 wt% Pt cocatalyst loaded *via* photodeposition was used as the photocatalyst (see Fig. S2 for the X-ray diffractometry [XRD] pattern of TiO_2). A flow-type cell was used (Fig. S3), and the Cl_2 produced was trapped as ClO^- ions in 4 M NaOH *via* disproportionation (Eq. 5). The detailed experimental procedure is shown in the Supporting Information.

A 500 mM aqueous NaCl solution was prepared as a model seawater/brine sample, in this study. Subsequently, the gas evolution reaction in brine was monitored over time at different pH values under 365 nm light irradiation (Fig. 2(A)). Under acidic condition (pH 1), H_2 and Cl_2 were preferentially produced, although a small amount of O_2 was also evolved. After the LED light was switched off, the amount of Cl_2 continuously increased gradually for an additional 45 min and then saturated. This delay was mainly caused by slow bubbling in the flow system (5 mL min^{-1}). Furthermore, the e^-/h^+ ratio of the products—which was initially 3.4—decreased with time and eventually reached almost unity (Fig. S4), indicating that the reaction proceeded in a stoichiometric manner. After the reaction, no HClO or ClO^- was detected in the reaction cell. In addition, some control experiments clearly show that Pt-loaded TiO_2 photocatalyst is necessary to produce H_2 and Cl_2. (See Table S1)

Contrary, in a closed batch system, H_2 production was stopped after 1 h (Fig. S5). Therefore, backward reactions such as $H_2 + 1/2O_2 \rightarrow H_2O$ and $H_2 + Cl_2 \rightarrow 2HCl$ were largely suppressed owing to the use of the flow-type reaction cell.

After the reaction for 1 h, there was no change in the crystalline phase in XRD (Fig. S6). On the other hand, XPS and SEM showed a clear difference in Figs. S7 and S8, respectively. Although the Pt signal was observed after the reaction in XPS, the peak intensity has largely reduced, indicating that Pt species were partially dissolved after 1 h. SEM images in Fig. S8 showed aggregation of Pt particles after the reaction, which may contribute to the reduction of the intensity in XPS.

Under neutral condition, H_2 and a small amount of O_2 evolved steadily, whereas Cl_2 and HClO were not detected by colorimetry. Moreover, the e^-/h^+ ratio of the final product for this scenario was not apparently unity. HClO and NaClO can absorb 365 nm light, which suggests that photolysis should occur under these UV irradiation conditions. It was reported

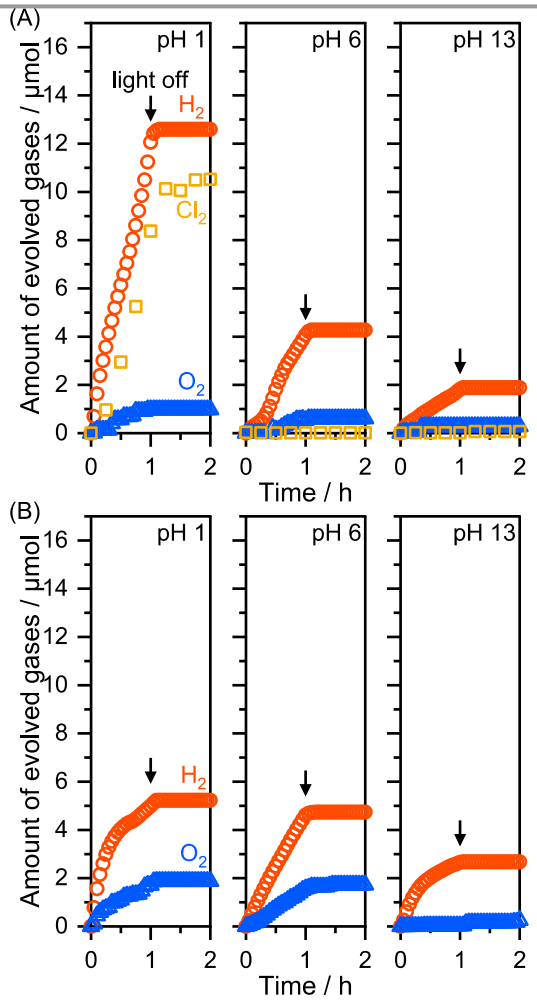

Fig. 2 Time courses of (A) brine splitting and (B) water splitting using 0.1 wt% Pt-loaded TiO_2 under different pH conditions. Reaction conditions: catalyst, 10 mg; solution, 500 mM NaCl aq. or water (30 mL, pH adjusted with eighter $HClO_4$ or NaOH); light source: 365 nm LED.

that ClO^- decomposes *via* the reaction $2ClO^- \rightarrow 2Cl^- + O_2$.[19,20] However, in this case, O_2 should be evolved and pure water splitting should proceed as a total reaction. Ion chromatography confirmed the production of ClO_3^- and Cl^- under UV irradiation, as reported previously,[17] suggesting that the photolysis of HClO or ClO^- to ClO_3^- likely occurred, as follows:

$$3ClO^- \rightarrow ClO_3^- + 2Cl^- \quad (7)$$

HClO was detected in the reaction cell when the reaction solution was analyzed 3 min after being irradiated. Furthermore, ion chromatography suggested that almost all the HClO in the reaction cell converted to Cl^- and ClO_3^-. Therefore, H_2 and HClO were presumably generated stoichiometrically at one time in the reaction cell, but HClO decomposed and converted to ClO_3^-, instead of being removed from the reaction cell as Cl_2 *via* Eq. 5, resulting in almost no O_2 and Cl_2 in the flow-type reactor. Although certain studies have hinted at the possibility of HClO decomposition, no investigation has confirmed the balance between reduction and oxidation. Our results indicated that the e^-/h^+ ratio was unity for the reaction conducted in neutral as well as acidic media, which was vital for certifying the steadiness of the catalysis. A similar phenomenon was observed in the scenario with a basic solution (pH 13).

Notably, the H_2 production rate was higher at a lower solution pH. It is known that the potential of the valence band maximum shifts with changes in pH, resulting in a larger driving force for Cl^- oxidation at lower pH (Fig. S1), which led to higher Cl_2 evolution activity. Additionally, higher H^+ concentration likely reduced the overpotential for H_2 production on the Pt surface.

For comparison, time courses of water splitting without NaCl were investigated under the aforementioned pH conditions (Fig. 2(B)). In the neutral medium (pure water), H_2 and O_2 evolved stably in a stoichiometric manner ($H_2/O_2 = 2$). When the pH was tuned to 1, the evolution rate initially increased—similar to that in the brine splitting at pH 1—and then gradually decreased. The activity did not recover even when the reaction cell was re-purged with Ar gas (Fig. S9), indicating irreversible degradation at pH 1. The factors underlying this degradation at acidic pH without NaCl could not be clarified; notably, the surface of TiO_2 could have changed marginally during the reaction. Only H_2 evolution was detected from the basic solution, as observed previously in water splitting reactions.[21,22] Although the detailed reasons are not fully understood, one of the possibilities is the formation of alternative oxidative products, such as H_2O_2, and another possibility is that in cases of low activity, O_2 was not detected due to the relatively low sensitivity to O_2. The non-stoichiometry of this system warrants further investigation.

Notably, the maximum H_2 production rate in acidic brine (12.7 μmol h^{-1}) was higher than that in pure water (4.7 μmol h^{-1}). The addition of NaCl is known to reduce the H_2 production rate under neutral conditions (Table S2). Therefore, a higher H_2 production rate can be achieved *via* brine splitting by adjusting the pH, even though the oxidation potential of Cl^- is more positive than that of water.

The photocatalyst enabled steady, linear production of H_2 and Cl_2 for more than 10 h (Fig. 3). After 14 h, the concentration

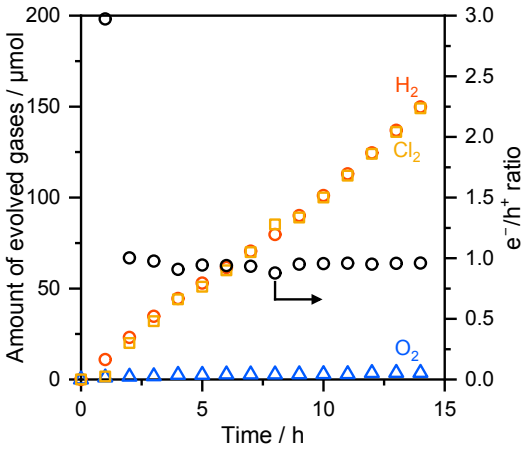

Fig. 3 Time-dependent gas evolution through brine splitting with 0.1 wt% Pt-loaded TiO_2. Reaction conditions: catalyst, 10 mg; solution, 500 mM NaCl aq. (30 mL, pH 1); light source: 365 nm LED. Circular, square-shaped, and triangular datapoints indicate H_2, Cl_2, and O_2, respectively.

of ClO^- in the trap solution exceeded 4 mM, which was sufficient for disinfection-related applications.[23] Although O_2 evolved slightly during the initial stage of the reaction, as shown in Fig. 2(A), it became negligible after 5 h. This result indicates that the Cl^- ion oxidation preferentially occurred even though O_2 was thermodynamically preferred as the product over Cl_2.

Despite the partial dissolution of the Pt species after 1 h as mentioned above, steady H_2 and Cl_2 evolution was confirmed over 10 h, and no H_2 was observed without Pt-modification (Table S1, entry 4). Therefore, it is likely that the remaining Pt species were stably active for brine splitting.

Photoelectrochemical measurements were conducted in the acidic medium to elucidate the effect of Pt cocatalyst on oxidation reaction. TiO_2/Ti photoelectrode was prepared by calcination of Ti substrate. Detailed experimental procedures and characterization are presented in Supporting Information. The selectivity (faradaic efficiency for Cl_2) of a TiO_2 photoelectrode toward Cl_2 evolution was not affected by Pt loading (TiO_2 and Pt-loaded TiO_2 photoelectrodes were 59% and 60%, respectively.). Pt was considered to act as a cocatalyst for H_2 evolution and not participate in oxidation. Therefore, the TiO_2 surface presumably provided active sites for oxidation.

Notably, the faradaic efficiency for Cl_2 was lower than in the suspension-based system, although no O_2 was detected during the process. One reason for this is the decomposition of HClO. The large dimensions of the photoelectrode (2 × 3 cm^2) prevented the removal of Cl_2 gas from the surface, consequently promoting photolysis and reducing selectivity. Another potential reason is the direct production of oxidizing species such as ClO_3^-.

Density functional theory (DFT) calculations were performed to scrutinize the kinetic aspects governing the selectivity for O_2/HClO production.[24–30] Using a commonly accepted theoretical description involving four proton-coupled electron-transfer (PCET) steps with two H_2O molecules,[31–36] the mechanisms underlying intermediate formation and oxidation of HCl and H_2O were investigated using the $Ti(OH)_2$–O_2–$Ti(OH)_2$ cluster model for rutile TiO_2.[34,35,37] The DFT results indicated

that the first deprotonation step from the adsorbed HCl or H_2O was the rate-limiting step for both reactions, similar to those reported previously for H_2O oxidation (Figs. S10 and S11).[31,33,36] The Δ*G* value of the rate-limiting step for HCl (2.20 eV; Table S3) was lower than that for H_2O (2.40 eV; Table S3), implying that the HCl oxidation was kinetically favorable.

The estimated apparent quantum yield of the entire brine splitting reaction in the acidic medium (~0.6% at 365 ± 20 nm) is comparable to that reported previously for TiO_2-photocatalyzed water splitting.[38] Additionally, the calculated turnover number for H_2PtCl_6 (~10^3) indicated that Cl_2 was produced from the Cl^- ions in the solution. Therefore, our results establish the credentials of a new artificial photosynthesis system that can simultaneously produce H_2 and Cl_2 from brine.

Although simultaneous production of H_2 and Cl_2 in acidic media is a noteworthy reaction, it requires an acid feed to maintain pH and supply protons for consumption. Therefore, in practical settings, this system should be equipped with an acid-wasting process. On the other hand, the production of ClO^- and H_2 in basic media does not change pH. Therefore, the development of photocatalysts that can split brine in basic media is more feasible than that in acidic environments, despite being more challenging owing to its higher Δ*G* value.

Additionally, visible-light-responsive photocatalysts that can exhibit high efficiency as well as suppress the decomposition of HClO and ClO^- under UV light must be developed.

In summary, Pt-loaded TiO_2 was shown to split brine into H_2 and Cl_2 in a stoichiometric manner under UV irradiation in the flow-type reactor. Essentially, an innovative artificial photosynthesis system was designed by combining the production of H_2 with that of high-value-added Cl_2 instead of O_2. Cl_2 was preferentially produced with a selectivity of ~100% for more than 10 h. Furthermore, the H_2 evolution rate of acidic brine splitting was higher than that of pure water splitting, resulting in a more efficient conversion of sunlight. We believe that our findings will help enrich the field of photocatalytic brine splitting and boost the practical viability of photocatalytic H_2 production systems.

Conflicts of interest

There are no conflicts to declare.

References

1 J. Rogelj, M. den Elzen, N. Höhne, T. Fransen, H. Fekete, H. Winkler, R. Schaeffer, F. Sha, K. Riahi and M. Meinshausen, *Nature*, 2016, **534**, 631–639.
2 H. D. Matthews and S. Wynes, *Science*, 2022, **376**, 1404–1409.
3 J. Whitehead, P. Newman, J. Whitehead and K. L. Lim, *Sustainable Earth Rev.*, 2023, **6**, 1.
4 C. Klassert, J. Yoon, K. Sigel, B. Klauer, S. Talozi, T. Lachaut, P. Selby, S. Knox, N. Avisse, A. Tilmant, J. J. Harou, D. Mustafa, J. Medellín-Azuara, B. Bataineh, H. Zhang, E. Gawel and S. M. Gorelick, *Nat Sustain*, 2023, **6**, 1406–1417.
5 R. K. B. Karlsson and A. Cornell, *Chem. Rev.*, 2016, **116**, 2982–3028.
6 S. Okunaka, Y. Miseki and K. Sayama, *iScience*, 2020, **23**,101540.
7 H. Komiya, T. Shinagawa and K. Takanabe, *ChemSusChem*, 2022, **15**, e202201088.
8 T. P. Keane, S. S. Veroneau, A. C. Hartnett and D. G. Nocera, *J. Am. Chem. Soc.*, 2023, **145**, 4989–4993.
9 W. A. Rutala and D. J. Weber, *Clin. Microbiol. Rev.*, 1997, **10**, 597–610.
10 R. Mikutta, M. Kleber, K. Kaiser and R. Jahn, *Soil Sci. Soc. Am. J.*, 2005, **69**, 120–135.
11 L. Wang, M. Bassiri, R. Najafi, K. Najafi, J. Yang, B. Khosrovi, W. Hwong, E. Barati, B. Belisle, C. Celeri and M. C. Robson, *Journal of Burns and Wounds*.
12 K. Sayama, *ACS Energy Lett.*, 2018, **3**, 1093–1101.
13 S. Iguchi, Y. Miseki and K. Sayama, *Sustainable Energy Fuels*, 2018, **2**, 155–162.
14 S. Okunaka, Y. Miseki and K. Sayama, *Catal. Sci. Technol.*, 2021, **11**, 5467–5471.
15 R. Pang, Y. Miseki and K. Sayama, *Catal. Sci. Technol.*, 2022, **12**, 2935–2942.
16 Y. Shiraishi, Y. Shimabukuro, K. Shima, S. Ichikawa, S. Tanaka and T. Hirai, *JACS Au*, 2023, **3**, 1403–1412.
17 K. Maeda, H. Masuda and K. Domen, *Catal. Today*, 2009, **147**, 173–178.
18 X. Guan, F. A. Chowdhury, N. Pant, L. Guo, L. Vayssieres and Z. Mi, *J. Phys. Chem. C*, 2018, **122**, 13797–13802.
19 M. J. Watts and K. G. Linden, *Water Res.*, 2007, **41**, 2871–2878.
20 K. Mase, M. Yoneda, Y. Yamada and S. Fukuzumi, *Nat Commun*, 2016, **7**, 11470.
21 T. Hisatomi, T. Yamamoto, Q. Wang, T. Nakanishi, T. Higashi, M. Katayama, T. Minegishi and K. Domen, *Catal. Sci. Technol.*, 2018, **8**, 3918–3925.
22 K. Watanabe, A. Iwase and A. Kudo, *Chem. Sci.*, 2020, **11**, 2330–2334.
23 E. W. Rice, R. M. Clark and C. H. Johnson, *Emerging Infect. Dis.*, 1999, **5**, 461–463.
24 M. J. Frisch, G. W. Trucks, H. B. Schlegel, *et. al*, *Gaussian 16, Revision C.02*, Gaussian, Inc., Wallingford CT, 2019.
25 A. D. Becke, *J. Chem. Phys.*, 1993, **98**, 5648–5652.
26 C. Lee, W. Yang and R. G. Parr, *Phys. Rev. B*, 1988, **37**, 785–789.
27 R. Krishnan, J. S. Binkley, R. Seeger and J. A. Pople, *J. Chem. Phys.*, 1980, **72**, 650–654.
28 P. J. Hay, *J. Chem. Phys.*, 1977, **66**, 4377–4384.
29 H. Kusama, M. Kodera, K. Yamashita and K. Sayama, *Phys. Chem. Chem. Phys.*, 2022, **24**, 5894–5902.
30 X. Zhang, Y. Liu, X. Ma, F. Jin, B. Abulimiti and M. Xiang, *Optik*, 2020, **221**, 165395.
31 Á. Valdés, Z.-W. Qu, G.-J. Kroes, J. Rossmeisl and J. K. Nørskov, *J. Phys. Chem. C*, 2008, **112**, 9872–9879.
32 J. Yang, D. Wang, X. Zhou and C. Li, *Chem. Eur. J.*, 2013, **19**, 1320–1326.
33 M. Z. Ertem, N. Kharche, V. S. Batista, M. S. Hybertsen, J. C. Tully and J. T. Muckerman, *ACS Catal.*, 2015, **5**, 2317–2323.
34 F. Rodríguez-Hernández, D. C. Tranca, B. M. Szyja, R. A. van Santen, A. Martínez-Mesa, Ll. Uranga-Piña and G. Seifert, *J. Phys. Chem. C*, 2016, **120**, 437–449.
35 F. Rodríguez-Hernández, D. C. Tranca, A. Martínez-Mesa, Ll. Uranga-Piña and G. Seifert, *J. Phys. Chem. C*, 2016, **120**, 25851–25860.
36 X. Zhou and H. Dong, *J. Phys. Chem. C*, 2017, **121**, 20662–20672.
37 H. Kusama, M. Kodera and K. Sayama, *ChemistrySelect*, 2023, **8**, e202300114.
38 K. Maeda, *Chem. Commun.*, 2013, **49**, 8404–8406.